Modeling of a Solar Heat for Industrial Processes (SHIP) System using Fresnel Collectors

Marco A. David-Hernández, Antonio Cazorla-Marín, José Gonzálvez-Maciá, Jorge Payá

Instituto Universitario de Investigación en Ingenieria Energética

Universitat Politècnica de València

Camino de Vera s/n, 46022, Valencia, Spain

Abstract

A quasi-dynamic model has been developed to simulate the dynamics and energy performance of a Solar Heat for Industrial Process (SHIP) system with Fresnel collectors under different control schemes and with variable heat demand. The model validation has been carried out with measurements obtained from the SOLPINVAP experimental facility in Almassora (Spain) during the summer of 2021 and 2022. This facility comprises a modular Fresnel collector solar field and a kettle reboiler. The results show that the predicted energy generation is in the same order of magnitude as in the measurements, and the overall system dynamics are reproduced accurately.

Keywords: Solar Heat for Industrial Process, Modelling, Fresnel collector, Quasi-dynamic model

1. Introduction

Solar Heat for Industrial Process (SHIP) is the implementation of current and proven solar technologies to supply the heat demand needed in different manufacturing processes of the industry sector. The industrial sector represents one-third of the global energy demand, and SHIP systems have become a growing option for the decarbonization of this sector. SHIP systems have been pushed forward as an alternative to fossil fuel-based boilers. In these kinds of systems, predicting the components' behavior, dynamics, and performance under different demand, control conditions, and integration with the heat demand is of great interest.

In the field of SHIP, there are two main common technologies: non-concentrating, such as flat plate and evacuated tube collectors, and concentrating collectors for example parabolic trough and linear Fresnel. The industrial processes can be divided depending on the temperature level required by the process: low, medium and high temperature heat (Kumar, Hasanuzzaman and Rahim, 2019). Linear Fresnel collectors are commonly used to generate medium temperature heat ($150\ ℃ - 400\ ℃$). As reported in the Solar Heat World Wide report (Weiss and Spörk-Dür, 2022), by the end of March 2022 SHIP plants by collector type in operation there are 20 linear Fresnel collectors SHIP systems.

SHIP systems are used to harness the incident irradiance from the sun and deliver it in the form of heat to an industrial process. The useful heat is transmitted by means of a heat transfer fluid, which usually is thermal oil, water, or steam. In this field, experimental on-site documentation of SHIP systems using linear Fresnel collectors is rather limited, being the case of a pharmaceutical plant in Jordan (Berger *et al.*, 2016) the one with more documentation.

In the present work, a quasi-dynamic model that simulates the dynamics and performance of a SHIP system, with a modular Fresnel collector solar field and a modified kettle reboiler, has been developed within the frame of the SOLPINVAP project (INDERTEC, 2020). Experimental measurements have been carried out during the summer of 2021 and 2022 at the experimental facility SOLPINVAP, located in Almassora, Spain. Two measured days have been selected based on the measured irradiance. Simulations with the characteristics and control parameters of the SOLPINVAP solar field have been carried out with the developed model. The validation of the developed model with the simulation results and the measurements of the selected days is shown in the following sections.

Selection and/or peer review under responsibility of Scientific Committee
doi:10.18086/eurosun.2022.05.03 Available at http://proceedings.ises.org

2. Methodology

2.1. System Model

A mathematical quasi-dynamic model has been developed and built inside the object-oriented programming environment of MatLab. The latter was selected as modeling software due to its built-in libraries capable of solving differential algebraic equations systems (DAE). Each physical component has been programmed as an individual object with a set of equations, inputs, and outputs. The reason for using objects is to give the model the flexibility to assemble a system with any number of components and connections scheme.

The present work analyzed a system that comprises a shell and tube heat exchanger named kettle reboiler, a modular Fresnel collector solar field, a circulation pump, a filling pump, a steam extraction valve, and pipelines. In Fig. 1, the system components are represented with their thermodynamic interface (dots) between objects.

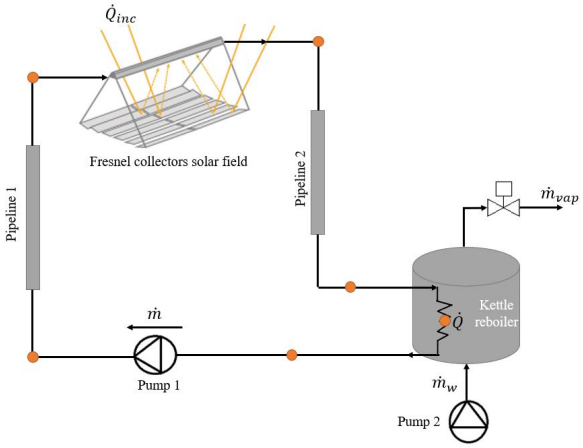

Fig. 1: System diagram with the model components on Indirect Steam Generation mode

Pressurized water has been used as heat transfer fluid throughout the solar field. The REFPROP library (NIST, 2013) has been included in MatLab to calculate the thermodynamic properties of the fluid. The main components shown in Fig. 1 are explained in the following sections.

2.2. Kettle Reboiler Model

The kettle reboiler installed at the experimental platform has been modified to work in two modes: Indirect Steam Generation (ISG) and Direct Steam Generation (DSG). It has two main functions: to separate the liquid water from steam and to accumulate energy.

Complex models for a tank with a 2-phase working fluid can be found in the literature. Such models consider the 2-phase fluid as two separate fluids. Thus, the thermodynamic state of each phase is known at any given time step (Stevanovic, Maslovaric and Prica, 2012). These models are helpful when the steam and liquid water have different temperatures. However, in SHIP systems, that is rarely the case. In this work, a simplified tank model has been developed, where the 2-phase fluid inside the kettle reboiler is considered in thermodynamic equilibrium at each time step. Thus, the thermodynamic state of the 2-phase fluid can be known by calculating two independent properties. The properties selected for the calculation are its density ρ and specific internal energy u, as shown in equations (eq. 1) to (eq. 3). Furthermore, the kettle reboiler has been assumed as a cylinder for simplification purposes.

$$\frac{d\rho}{dt} = \frac{\sum \dot{m}_{in} - \sum \dot{m}_{out}}{V_T} \quad \text{(eq. 1)}$$

$$\frac{dU}{dt} = \dot{Q}_{in/out} + \sum(\dot{m}_{in} \cdot h_{in}) - \sum(\dot{m}_{out} \cdot h_{out}) \quad \text{(eq. 2)}$$

$$U = \rho \cdot V_T \cdot u + M_M \cdot C_{p,M} \cdot T_M \quad \text{(eq. 3)}$$

The kettle reboiler is modeled with a differential-algebraic equations system. Where (eq. 3) represents the total internal energy of the tank: the sum of the energy of the 2-phase fluid and the tank's mass. V_T is the total internal volume of the kettle reboiler, M_M and $C_{p,M}$ are the tank material's mass and specific heat, respectively. In (eq. 1), $\dot{m}_{in}$ and $\dot{m}_{out}$ are the inlet and outlet mass flow rates, respectively. On the right-hand side of (eq. 2), $\dot{Q}_{in/out}$ represents any heat flow rate going into/out the kettle reboiler, for example, input heat from the shell and tube heat exchanger or heat loss to the ambient. It has been assumed that, when the fluid is in saturation state, the temperature

of the tank material, T_M, is the same as the temperature of the fluid inside the tank. Then, this temperature can be calculated as a function of the density and the specific internal energy of the 2-phase fluid: $T_M = T_{fl} = f(\rho, u)$.

2.3. Fresnel Collector Model

The Fresnel module collector model has been created as a black box, where the inputs were reduced to weather data and inlet mass flow, enthalpy, and pressure of the flowing water.

A pyranometer for the measurement of global horizontal irradiance has been installed at the experimental plant. However, there is no other instrument to measure or calculate the direct normal irradiance (DNI). Thus, on the lack of this information, a clear-sky model has been implemented to estimate the DNI. In the present work, the selected model is the clear-sky model presented in the ASHRAE handbook (ASHRAE, 2013). The disadvantage of this methodology is that it works on the assumption of a clear atmosphere.

A simple Incident Angle Modifier (IAM) based model has been implemented to calculate the incident heat on the collector absorber. The longitudinal and transversal IAM (IAM_l and IAM_t respectively) were calculated with the Monte Carlo Ray Tracing software tool Tonatiuh (CENER, 2017). Thus, the incident heat on the absorber tube can be calculated as shown in (eq. 4) (Morin *et al.*, 2012). Where A is the total reflective effective aperture area on the horizontal plane of a Fresnel module, N_{mod} is the number of modules, and Cl is a factor related to the cleanliness of the reflective surface.

$$\dot{Q}_{inc} = \eta_0 \cdot IAM_l \cdot IAM_t \cdot Cl \cdot A \cdot N_{mod} \cdot DNI \quad \text{(eq. 4)}$$

No thermal inertia is considered in the Fresnel collector model, as the developed quasi-dynamic model assumes that the thermal inertia is concentrated in the kettle reboiler.

2.4. Heat Loss Model

A simple thermal loss model has been used for the pipelines and the kettle reboiler. Both components have been assumed to be cylinders. The heat loss depends on the temperature difference ΔT between the temperature of the fluid and the ambient temperature, as shown in equation (eq. 5), where R_t is the thermal resistance. The model is used to simulate the thermal loss of each component throughout the simulation. The heat loss through the walls on both bases of the cylinder is also considered in the kettle reboiler.

$$\dot{Q}_{loss} = \frac{\Delta T}{R_t} \quad \text{(eq. 5)}$$

3. Experimental Facility

The experimental solar platform, SOLPINVAP, is located in Almassora, Spain (39.958, -0.074). The facility is comprised of a single row of 6 collector modules in series. There is a total of 9 absorber tubes for a total length of $35.12\ m$. The Fresnel solar collector modules have been manufactured by Solatom (Solatom CSP, 2018). Each module has a reflective aperture area of $26.4\ m^2$. The optical efficiency of the Fresnel modules, calculated with Tonatiuh, is $\eta_0 = 66.7\%$. The kettle reboiler is located inside a skid structure on the southern side of the solar field. The solar field is north-south oriented with a deviation of $32°$ northeast (being north $0°$ and south $180°$). In Fig. 2 a) and b), the Fresnel solar field and the kettle reboiler are shown.

a) b)

Fig. 2: Photos taken at the SOLPINVAP experimental plant, where in a) the Fresnel module collector field and in b) the kettle reboiler inside the skid

3.1. Control Parameters of the Solar Field

The circulation pump of the primary circuit of the solar field is turned on when the global irradiance, measured by the pyranometer, is greater than $150\ W/m^2$. It is turned off when there is not enough irradiance or when the measured liquid water level inside the tank is lower than a critical level of $-80\ mm$ (where $0\ mm$ is at the center of the kettle reboiler). The level inside the tank is kept between a maximum and minimum value by filling the tank with treated water.

The steam extraction is carried out by controlling the aperture of two pneumatic valves. The first valve keeps the pressure inside the tank, and the second keeps the pressure inside an expansion tube. The latter has the function of imitating the demand side (with a constant process pressure). In the skid installation, a flow meter has been added to measure the steam mass flow rate, as shown in Fig. 3.

Fig. 3: Steam mass flow meter installed at the extraction side of the skid

4. Results and Discussions

As mentioned in section 2.2, the solar field SOLPINVAP was designed to work on ISG and DSG modes. Two measurement campaigns on the ISG mode have been carried out at the experimental solar plant SOLPINVAP to validate the developed model. In ISG mode, the kettle reboiler receives the heat absorbed from the solar field through the tube heat exchanger.

The first measurements were done during the summer of 2021, and the following measurements were acquired during the summer of 2022. Two separate days are analyzed in the present work, one from each campaign. The first is June 24, 2021, and the second on June 12, 2022.

4.1. Weather Data

In Fig. 4 the global, direct normal, and diffuse irradiance for both June 24, 2021, and June 12, 2022, are shown as

reported in the measurements from the Valencia airport in Manises. Although the SOLPINVAP facility is 63 km away from Valencia Airport, it has been assumed that the weather does not significantly change around the same region.

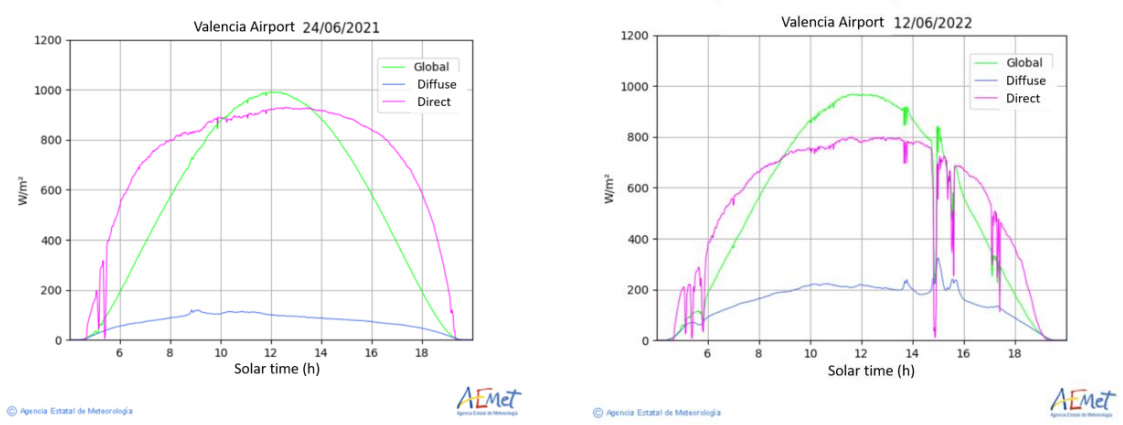

a) b)

Fig. 4: Global (green), direct normal (magenta) and diffuse (blue) irradiance measured at Valencia airport for a) June 24, 2021 and b) June 12, 2022 (taken from the Agencia Estatal de Meteorología – AEMET, Gobierno de España)

As shown in Fig. 4, both days presented a global irradiance with similar behavior to clear-sky conditions. Thus, the conditions are met for the use of a clear-sky model. As mentioned in section 2.3, the ASHRAE clear-sky model has been used for the calculations. The model uses optical depth indexes for the direct τ_b and diffuse τ_d irradiance, which depend on the location. These two indexes embody clear-sky conditions like precipitable water, aerosols, ozone, Etc. (ASHRAE, 2013). The optical depth indexes for both days have been estimated using the ASHRAE model, and the measurements are shown in Fig. 4. In Tab. 1 are listed the estimated optical depth indexes for each day, respectively.

Tab. 1: Optical depth indexes calculated with the clear-sky model and the irradiance measured at Valencia Airport

Optical Depth Index	June 24, 2021	June 12, 2022
τ_b(-)	0.4978	0.6969
τ_d(-)	2.4953	1.7500

In Fig. 5, the globlal irradiance measured by the pyranometer at the SOLPINVAP facility and the simulated irradiance, with the implemented clear-sky model using the optical depth indexes of Tab. 1, are shown. The root mean square error between the measured and simulated with the clear-sky model global irradiance on June 24, 2021 (Fig. 5 a)) is 16.05 W/m^2, whereas, on June 12, 2022 (Fig. 5 b)), the root mean square error is 69.9 W/m^2.

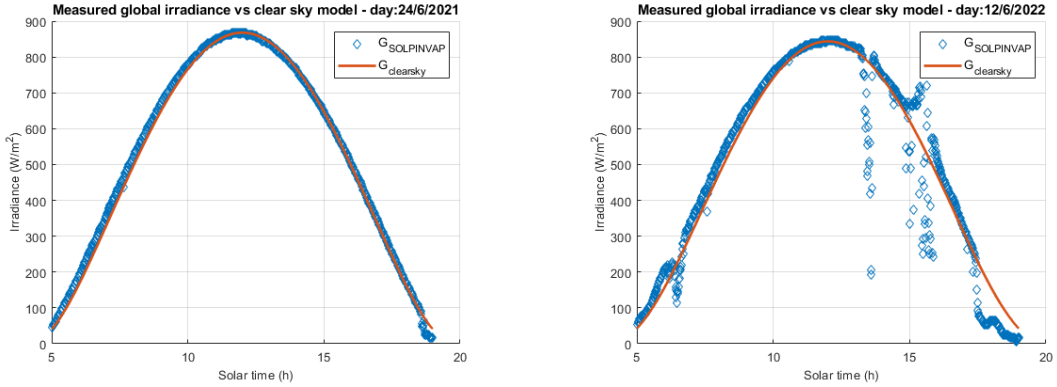

a) b)

Fig. 5: Global irradiance measured by the pyranometer at SOLPINVAP facility and the simulated with the clear-sky model and the respective optical depth indexes

4.2. Experimental Measurements

As mentioned above, two days are going to be analyzed in the present work. The measurements carried out during the two experimental campaigns at the SOLPINVAP plant are shown in Fig. 6. In both cases, the steam extraction was done through a steam valve controlled by a PID control scheme. Fig. 6 a) shows the temperatures at the inlet of the solar field $T1$ and the outlet $T2$, the temperature inside the kettle reboiler T_{tank}, the water level, and the measured steam mass flow rate at the extraction. The pressure inside the kettle reboiler is shown in Fig. 6 b). On June 24, 2021, solar energy was absorbed in the solar field, and there was steam extraction. The filling pump has turned on for 5 minutes during the measurements, as observed in Fig. 6 a). On June 24, 2021, the system was in function until the water level of the kettle reboiler reached a critical minimum. In Fig. 6 c) and d), the corresponding variables are shown on June 12, 2022. On June 12, 2022, solar energy was absorbed in the solar field, steam was extracted, and the water level control was active, as shown in Fig. 6 c).

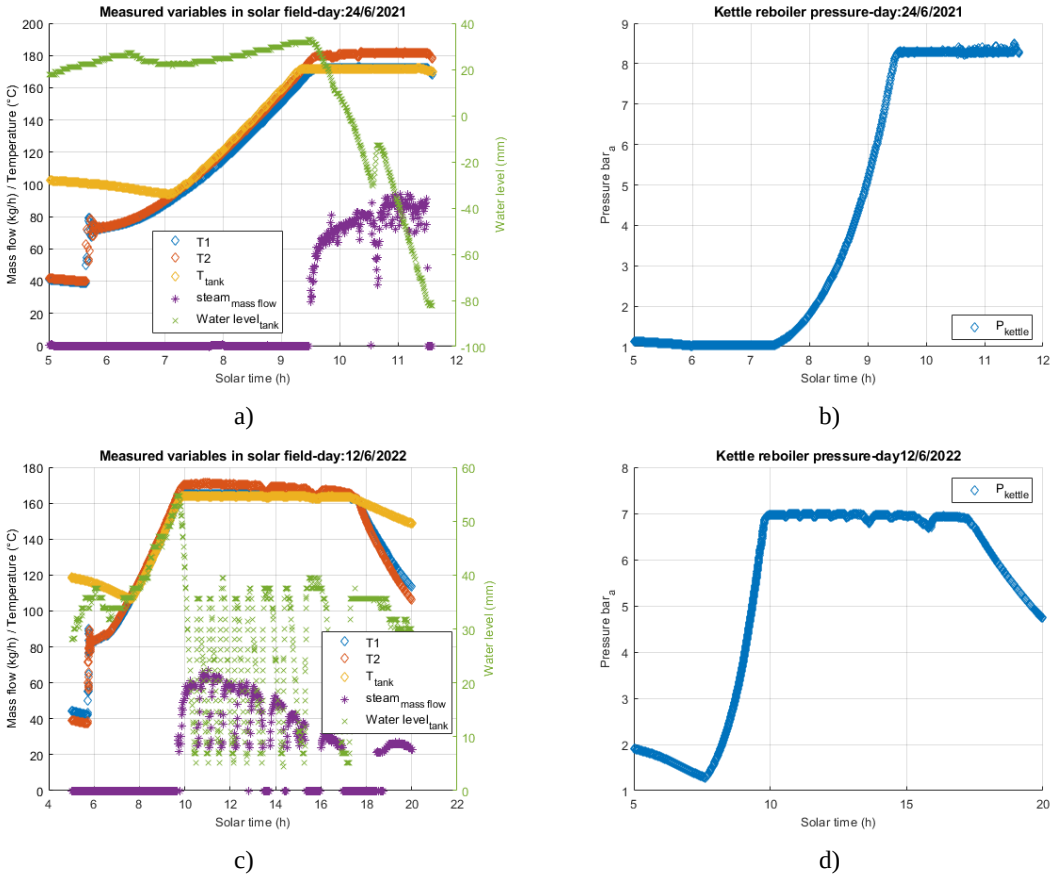

Fig. 6: Experimental measurements at SOLPINVAP. In a) and b) are the results on June 24, 2021, and in c) and d) the corresponding for June 12, 2022

The developed model is intended to simulate the system under normal working conditions with different control schemes and heat demands. In the following sections, the validation of the model with the experimental measurements of two days is presented, first on steady state and then on transitory and steady state. The DNI has been calculated during every time step with the optical depth indexes for the corresponding day and the clear-sky model.

4.3. Steady State

First, the Fresnel module collector model has been validated with the experimental measurements in the steady state period, i.e., a period where the temperature measurements in the solar field do not vary significantly. The inputs given to the model were the temperature at the inlet of the solar field, the water mass flow, and the clear-sky DNI. This validation was also used to estimate a clean factor for both measured days. Fig. 7 a) and b) present the validation results for June 24, 2021, and June 12, 2022, respectively, where $T2_{sim}$ and $T2_{exp}$ are the simulated and experimental temperatures, respectively, at solar field outlet. $T1_{exp}$ is the measured temperature at the inlet of the solar field, and $Mass\ flow_{solar\ field}$ is the mass flow rate of the pressurized water. On June 24, 2021 (Fig. 7 a)), the clean factor was estimated to be 70%, and the root mean square error between the simulated and measured solar field outlet

temperature was 0.3 K. It can also be observed that the model correctly follows the temperature tendency when there is a sudden change in water mass flow.

In the same way, the experimental measurements on June 12, 2022 (Fig. 7 b)) have been used to validate the Fresnel collector model. The estimated clean factor is 64%, and the root mean square error between the simulated and measured solar field outlet temperature is 0.19 K. In Fig. 7 b), decrements in the solar field inlet temperature and, consequently, at the outlet temperature can be observed. These decrements are due to the introduction of cold water when the filling pump is activated to increment the water level inside the kettle reboiler. Fig. 7 a) and b) also show no significant thermal inertia in the collector tubes.

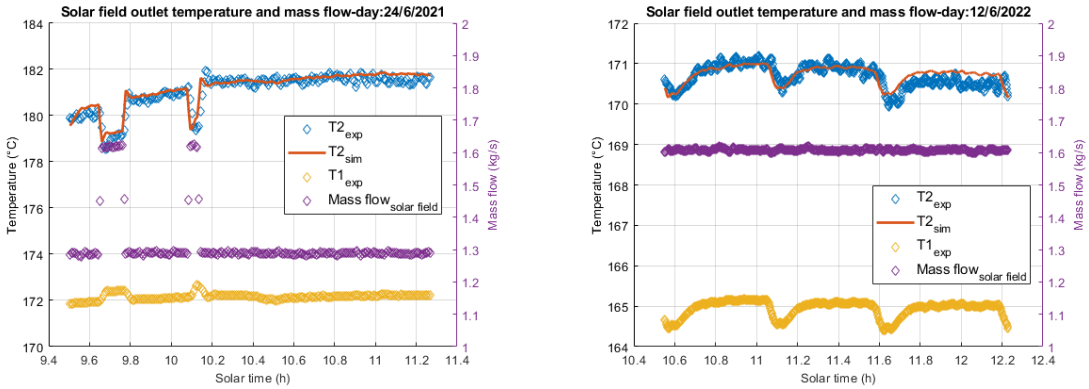

a) b)

Fig. 7: Predicted solar field outlet temperature, both simulated and measured, the solar field inlet temperature and water mass flow for: a) June 24, 2021 and b) June 12, 2022

The general model is then validated with the estimated clean factors in the same steady state time period. The general model is referenced as the complete system with all the components (see Fig. 1). The inputs to the general model are the weather data, the measured water mass flow rate, and control factors for steam extraction. A simple proportional control has been implemented to simulate the aperture of the steam extraction valve. Below, in Tab. 2, are listed the initial model parameters used for the simulation of the general model. As mentioned in section 3.1, the water level is referenced to the center of the kettle reboiler. Thus, a positive level value is above the center of the tank, and a negative value is below that point.

Tab. 2: Initial parameters for the simulation with the general model on steady state

Parameter	24/06/2021	12/06/2022	Unit
τ_b	0.4978	0.6969	-
τ_d	2.4953	1.7500	-
Clean Factor	70	64	%
Kettle Metal Mass	3079	3079	kg
Initial Kettle Pressure	8.1	6.9	bar_a
Initial Water Level	+25	+36	mm
Max Pressure	8.7	8.4	bar_a
Min Pressure	8	6	bar_a
Max Water Level	+10	+35	mm
Min Water Level	-81	+5	mm
Fill Water Temperature	50	50	℃

The comparison between the measured (subscript “exp”) and simulated (subscript “sim”) parameters of the solar

field in steady state are shown in Fig. 8. Where in Fig. 8 a) are the inlet and outlet solar field temperatures and water mass flow, Fig. 8 b) the kettle reboiler pressure and water level, and in Fig. 8 c) the extracted steam mass flow of June 24, 2021. In Fig. 8 d), e) and f), the respective comparison of the parameters mentioned before, on June 12, 2022, is graphed. In Tab. 3 are listed the corresponding root mean square error for each relevant variable for June 24, 2021 and June 12, 2022. Moreover, the relative difference between the experimental measured and simulated extracted energy is presented in Tab. 4. The generated energy is referred to as the integrated steam mass flow during the analyzed period.

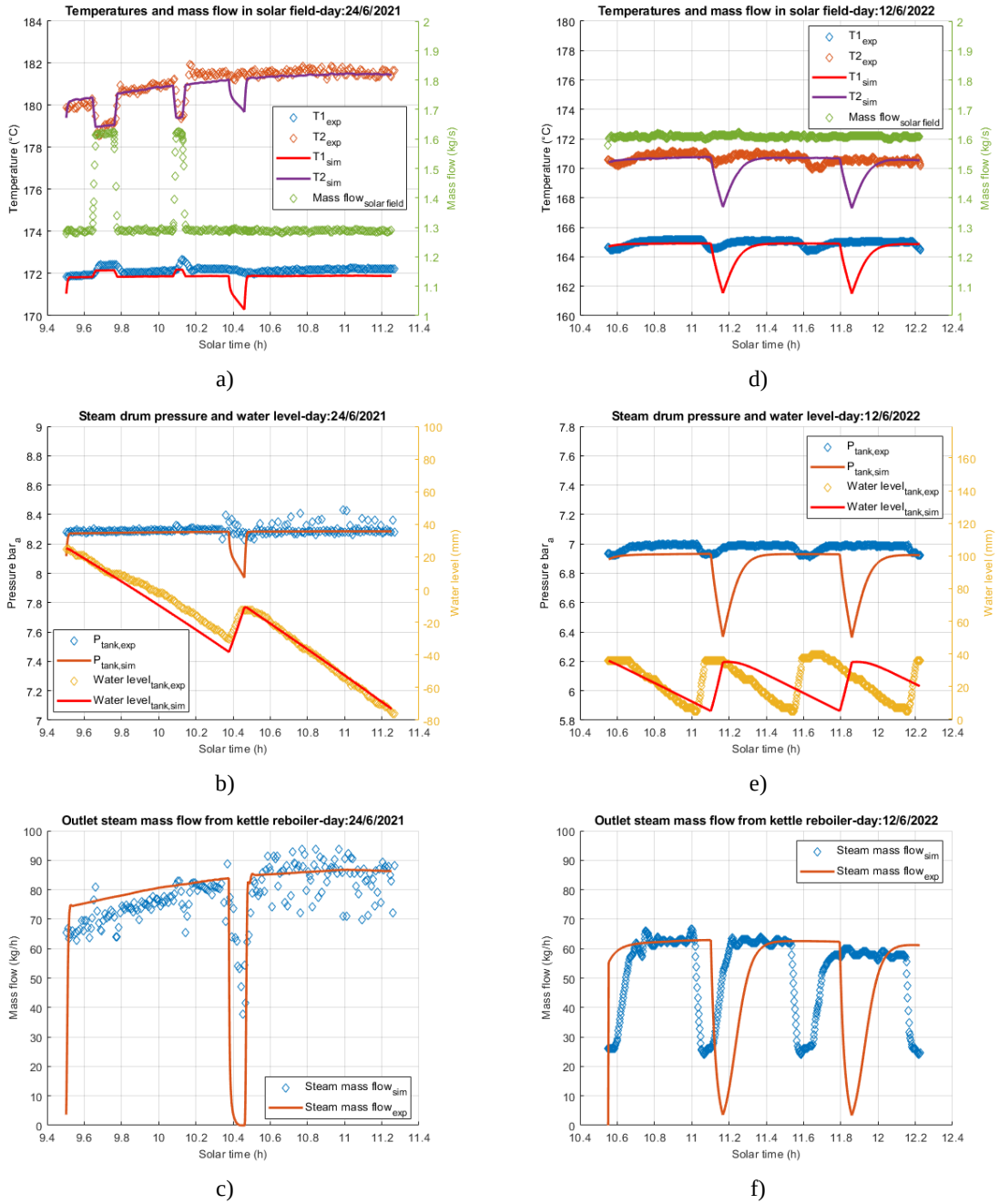

Fig. 8: Validation of the model on steady state time period. In a), b) and c) the results of June 24, 2021, and in d), e) and f) the simulation results of June 12, 2022 are shown.

Tab. 3: Root mean square error of the relevant parameters of two days in the analyzed time period

	Root Mean Square Error		
Parameter	**24/06/2021**	**12/06/2022**	**Unit**
$T1$	0.53	0.95	K
$T2$	1.02	0.91	K
P_{tank}	0.08	0.18	bar_a

Tab. 4: Comparison between measured and simulated generated energy in the analyzed time period

Parameter	**24/06/2021**	**12/06/2022**	**Unit**
Experimental Energy Extracted	380.52	241.2	MJ
Simulated Energy Extracted	378.43	242.32	MJ
Relative Difference	0.05	0.5	%

On both days, the filling pump introduced cold water into the kettle during the analyzed period. It can be observed how the model predicts a decrease in pressure greater than the measured by the pressure sensor, $0.31\ bar_a$ in the case of June 24, 2021 (Fig. 8 b)) and $0.56\ bar_a$ on June 12, 2022 (Fig. 8 e)). This is because the model considers a homogeneous 2-phase fluid inside the kettle reboiler; this means the 2-phase fluid is in thermodynamic equilibrium at every time step. However, this is not true in reality because there exists a stratification when cold water enters the tank. Nevertheless, the decrease in pressure predicted by the model does not significantly affect the energy generated by the system, as presented in Tab. 4.

4.4. Transient and Steady State

In this section, the model is validated with the experimental measurements, including the initial transient state of the system. The latter means when the day starts, and the pressurized water is heated up, and the kettle reboiler is pressurized up to the desired pressure level. The simulations in this section were carried out from the point where the inlet solar field temperature has reached $100\ ℃$, ensuring that the fluid inside the kettle reboiler is in saturation state.

In Tab. 5 are listed the initial parameters for the transient and steady state simulation. As mentioned before, on June 24, 2021, the main circulation pump and the system were turned off when the kettle reboiler water level reached a critical minimum. Thus, the simulation was carried out until that moment of the day. In the case of June 12, 2022, the simulation was done until there is presence of clouds, as observed in Fig. 5 b) and Fig. 6 c). The sky model does not simulate cloud presence. Therefore, the model validation was carried out just during the clear-sky section of the day.

Tab. 5: Initial parameters for the simulation with the general model on transient and steady state

Parameter	24/06/2021	12/06/2022	Unit
τ_b	0.4978	0.6969	-
τ_d	2.4953	1.7500	-
Clean Factor	70	64	%
Kettle Metal Mass	3079	3079	kg
Initial Kettle Pressure	1	1.28	bar_a
Initial Water Level	+23.6	+35.7	mm
Max Pressure	8.7	8.4	bar_a
Min Pressure	8	6	bar_a
Max Water Level	+10	+35	mm
Min Water Level	-81	+5	mm
Fill Water Temperature	50	50	℃

In Fig. 9, the validation of the general model, including the transient and steady state, with the measurements carried out on June 24, 2021, and June 12, 2022, is presented. Where the subscript "sim" stands for simulation and the subscript "exp" is for the experimental measurement. Fig. 9 a) and d) show the inlet and outlet solar field temperature and water mass flow. In Fig. 9 b) and e), the evolution of the pressure and water level throughout the day can be observed. Furthermore, the extracted steam mass flow on June 24, 2021, and June 12, 2022, is graphed in Fig. 9 c) and f) respectively, on each mentioned figure. The comparison between the measured and simulated extracted energy and the relative difference for both June 24, 2021, and June 12, 2022, is presented in Tab. 6.

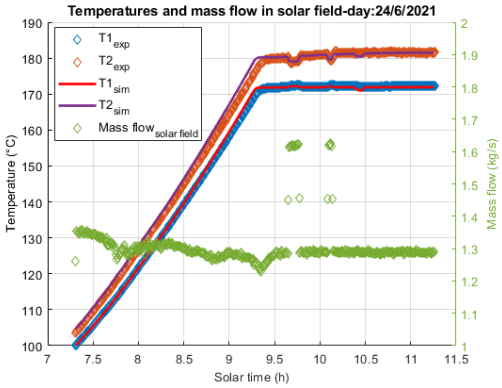

a)

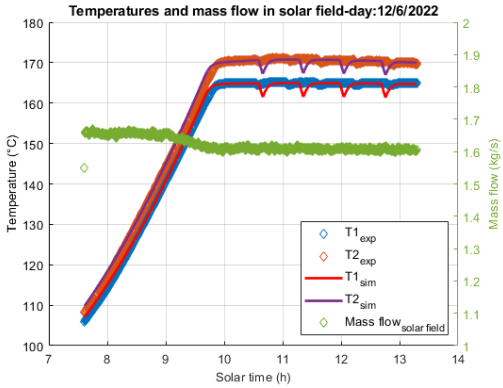

d)

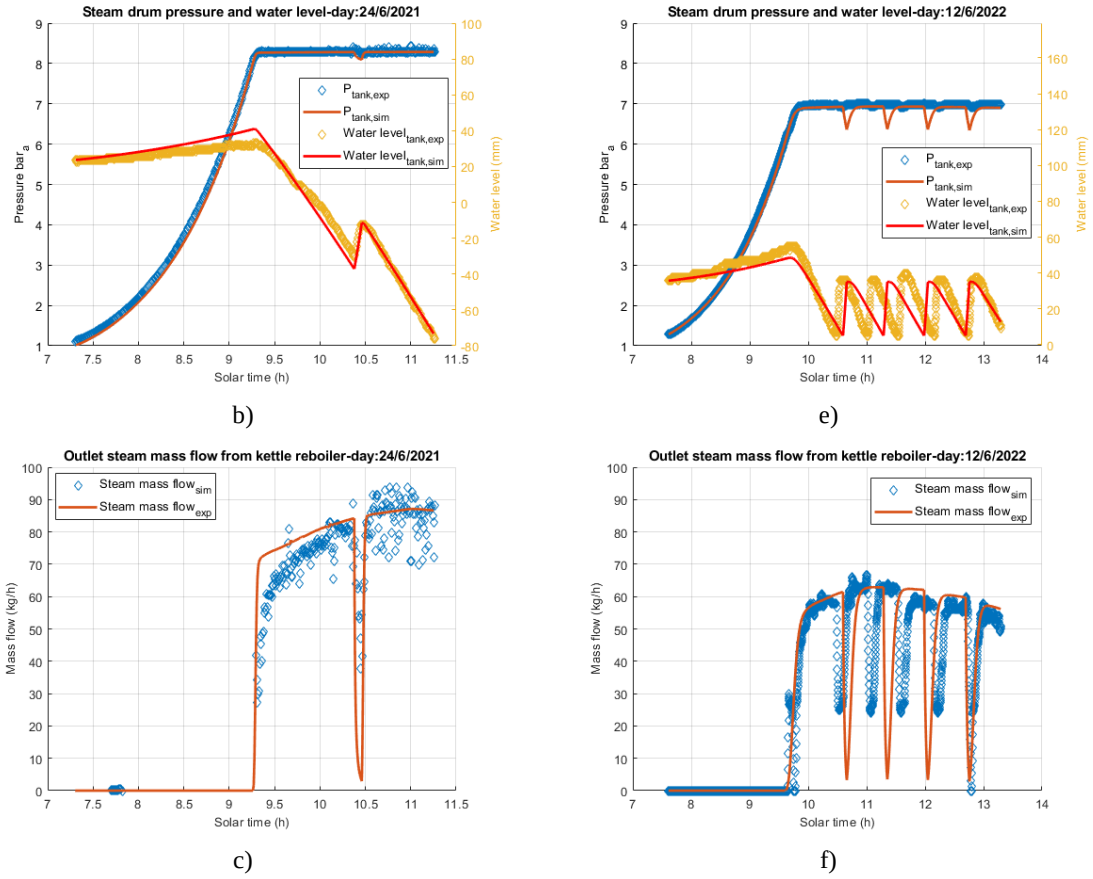

Fig. 9: Validation of the model on transient and steady state. In a), b) and c) the results of June 24, 2021, and in d), e) and f) the simulation results of June 12, 2022 are shown.

Tab. 6: Comparison between measured and simulated generated energy in the analyzed time period

Parameter	24/06/2021	12/06/2022	Unit
Experimental Energy Extracted	406.8	493.2	MJ
Simulated Energy Extracted	424.8	500.4	MJ
Relative Difference	4.4	1.5	%

Fig. 9 a), b), d), and e) show that, on both days and with their respective initial parameters, the model follows the tendency of the inlet and outlet solar field temperatures and the kettle reboiler pressure along the transient part of the day. During the steady state part of the simulation, the model predicts a decrease in pressure due to the introduction of cold filling water, as observed in Fig. 9 b) and e). The pronounced decrease of the simulated pressure occurs because the model does not account for stratification in the liquid phase when cold water is introduced. In Fig. 9 c) and f) shows that the simulated steam mass flow also decreases more than in reality when cold water fills the kettle reboiler. Nevertheless, as presented in Tab. 6, the latter does not significantly affect the final predicted energy generated by the system.

5. Conclusions

A quasi-dynamic model has been developed in MatLab that is able to simulate the dynamics, behavior, and performance of a SHIP system with a modular Fresnel collector solar field. The developed model simulates any collector module arrangement thanks to its object-oriented structure. It has been structured only to change few initial parameters considering weather data, the clean factor, and control variables. Thus, the rest of the parameters depend on the inputs mentioned before.

In order to estimate the DNI, measurements from the Valencia airport were used to estimate optical depth indexes

required for the implemented clear-sky model. The SHIP model has been validated with experimental measurements from the SOLPINVAP experimental platform during the summer of 2021 and 2022. The validation results show that the model correctly reproduces the temperatures and pressure tendencies in the transient and steady state. On steady state, the model simulates the solar field temperatures and pressure inside the kettle reboiler with small error. The model predicts a sudden pressure drop when cold water is introduced to the kettle reboiler, thus decreasing the predicted steam mass flow. The pressure drop may be smaller in reality because there is a stratification in the liquid phase when cold water enters the tank, and the same occurs with the extracted steam mass flow. However, it has been shown that the decrease in pressure does not significantly influence the simulated final energy generated compared with the experimentally measured energy generated.

Thus, the developed quasi-dynamic model is able to simulated accurately the behavior, dynamics, and performance and accurately predict the energy generated by a SHIP system that comprises a Fresnel collector solar field.

6. Acknowledgements

The authors gratefully acknowledge the company SolatomCSP, for all the information and operational data from the SHIP facility used in the present work, and for all the technical support. This work was partially supported by the Research and Development Aid Program (PAID-01-20) of the Universitat Politècnica de València for receiving the Research Fellowship FPI-UPV-2020. This publication has been carried out in the framework of the project "DECARBONIZACIÓN DE EDIFICIOS E INDUSTRIAS CON SISTEMAS HÍBRIDOS DE BOMBA DE CALOR", funded by the Spanish "Ministerio de Ciencia e Innovación (MCIIN)" with code number PID2020-115665RB-I00.

7. References

ASHRAE (2013) 'Handbook Fundamentals, Chapter 14. Climatic Design Information', *Atlanta*, 1952, pp. 1–56.

Berger, M. *et al.* (2016) 'First Year of Operational Experience with a Solar Process Steam system for a Pharmaceutical Company in Jordan', *Energy Procedia*, 91, pp. 591–600. Available at: https://doi.org/10.1016/j.egypro.2016.06.209.

CENER (2017) *Tonatiuh, Monte Carlo Ray Tracer Software*. Available at: https://iat-cener.github.io/tonatiuh/ (Accessed: 21 February 2022).

INDERTEC (2020) *Indertec desarrolla SOLPINVAP: Energía SOLar de Media Temperatura para procesos INdustriales con demanda de VAPor*. Available at: https://indertec.com/2020/01/19/indertec-desarrolla-solpinvap-energia-solar-de-media-temperatura-para-procesos-industriales-con-demanda-de-vapor/ (Accessed: 8 June 2020).

Kumar, L., Hasanuzzaman, M. and Rahim, N.A. (2019) 'Global advancement of solar thermal energy technologies for industrial process heat and its future prospects: A review', *Energy Conversion and Management*, 195(February), pp. 885–908. Available at: https://doi.org/10.1016/j.enconman.2019.05.081.

Morin, G. *et al.* (2012) 'Comparison of Linear Fresnel and Parabolic Trough Collector power plants', *Solar Energy*, 86(1), pp. 1–12. Available at: https://doi.org/10.1016/j.solener.2011.06.020.

NIST (2013) *REFPROP*. Available at: https://www.nist.gov/srd/refprop (Accessed: 23 September 2021).

Solatom CSP (2018) *SolatomCSP*. Available at: http://www.solatom.com/ (Accessed: 8 June 2020).

Stevanovic, V.D., Maslovaric, B. and Prica, S. (2012) 'Dynamics of steam accumulation', *Applied Thermal Engineering*, 37, pp. 73–79. Available at: https://doi.org/10.1016/j.applthermaleng.2012.01.007.

Weiss, W. and Spörk-Dür, M. (2022) 'Solar Heat World 2022. Global Market Development and Trends 2021. Detailed Market Figures 2020', p. 87. Available at: https://www.iea-shc.org/Data/Sites/1/publications/Solar-Heat-Worldwide-2021.pdf.